# HIGH-PERFORMANCE REVERSE OSMOSIS MEMBRANE ENABLED BY NANOFILLERS AND SURFACE MODIFICATION

A Thesis

by

YIFAN LIU

Submitted to the Office of Graduate and Professional Studies of
Texas A&M University
in partial fulfillment of the requirements for the degree of

MASTER OF SCIENCE

| | |
|---|---|
| Chair of Committee, | Choongho Yu |
| Committee Members, | Arum Han |
| | Svetlana Sukhishvili |
| Head of Department, | Ibrahim Karaman |

December 2016

Major Subject: Materials Science and Engineering

## ABSTRACT

With the rising demand for sustainably producing fresh water from saline sources, many researchers have been attracted to develop new reverse osmosis (RO) membranes with high water flux and salt rejection. Despite the great achievements researchers have made, there is still significant room for improving the water permeability and salt rejection of an RO membrane. Herein, we fabricated a RO membrane of advanced 3-layer structure and better performance both in anti-fouling and in water flux. This advanced membrane contains three layers with different modifications. The first modification was done by embedding zeolite and graphene oxide (GO) in the selective polyamide (PA) layer to introduce water flux channel. The second modification was an additional GO layer on the PA surface working as an anti-fouling layer. For final modification, we added a polyethylene glycol (PEG) layer which could serve to repel the organic foulant. The water permeability, salt rejection property, and anti-fouling ability of this new membrane have been investigated. We concluded that the combination of these structures led to an overall excellent RO performance which was supported by our experimental results.

## ACKNOWLEDGEMENTS

Firstly, I would like to thank my advisor, Dr. Yu, for his guidance and opinions during the whole period of my research. He pointed out a way of how to be a qualified graduate student for me when I missed my direction. Also, I want to thank my committee members, Dr. Han and Dr. Sukhishvili, for their help and feedback.

I especially thank my colleagues, Woongchul, Gang, and Suk Lae for helping me so much during the past two years. Also thanks to all other colleagues in the Nano Energy lab: Jui-Hung, Abdullah, Su-in, Henry, Burak, Jian, Dr. Kundo, and Hong.

Finally, I want to thank my family for their understanding and love during the past two years. I wouldn’t have been able to finish my degree without them.

## CONTRIBUTORS AND FUNDING SOURCES

This work was supervised by a thesis committee consisting of Professor Choongho Yu and Professor Svetlana Sukhishvili of the Department of Materials Science and Engineering and Professor Arum Han of the Department of Electrical and Computer Engineering

Graduate study was supported by a fellowship from Texas A&M University and a dissertation research fellowship from Qatar.

## NOMENCLATURE

| | |
|---|---|
| Reverse Osmosis | RO |
| Multi-stage flash distillation | MSF |
| Sea water reverse osmosis | SWRO |
| Brackish water reverse osmosis | BWRO |
| Polysulfone | PSF |
| Polyethersulfone | PES |
| Trimesoyl chloride | TMC |
| 1, 3-phenylene diamine | MPD |
| Linde type A | LTA |
| Bovine Serum Albumin | BSA |
| Interfacial Polymerization | IP |
| Fourier transform infrared | (FTIR) |

.

## TABLE OF CONTENTS

Page

ABSTRACT ..... ii

ACKNOWLEDGEMENTS ..... iii

CONTRIBUTORS AND FUNDING SOURCES ..... iv

NOMENCLATURE ..... v

TABLE OF CONTENTS ..... vi

LIST OF TABLES ..... viii

LIST OF SCHEMES ..... ix

LIST OF FIGURES ..... x

1. INTRODUCTION AND BACKGROUND ..... 1

1.1 Research background ..... 1
1.2 Mechanism of reverse osmosis desalination ..... 2
1.3 Approaches to increase membrane performance ..... 5
1.4 Motivation and experimental design ..... 9

2. CHEMICALS AND MATERIALS ..... 13

3. EXPERIMENTAL ..... 14

3.1 Zeolite preparation ..... 14
3.2 Preparation of PA layer with nanofillers ..... 14
3.3 Surface modification of PA layer with GO layer ..... 15
3.4 Surface modification of GO layer with PEG layer ..... 16
3.5 Characterization methods of nanofillers and membranes ..... 18
3.6 Performance and fouling characterization methods ..... 20

4. RESULTS AND DISCUSSION ..... 21

4.1 Characterization results of membranes..... 21
4.2 Membrane performance and antifouling properties ..... 27

5. CONCLUSION AND FUTURE WORK..... 36

REFERENCES..... 39

## LIST OF TABLES

Page

Table 1. List of samples ..... 18

Table 2. Contact angles of different samples ..... 26

Table 3. Comparison of RO membranes from literature ..... 38

## LIST OF SCHEMES

Page

Scheme 1. Schematic illustration of the 3-layer membrane ....10

Scheme 2. Schematic illustration of PEG anti-fouling layer.....12

Scheme 3. Schematic illustration of nanoparticles decoration.....15

Scheme 4. (a) TMC, (b) MPD, and (c) Schematic illustration of GO coating mechanism.....16

Scheme 5. Chemical structure of PEG modified GO.....17

## LIST OF FIGURES

Page

Figure 1. FTIR results of membranes with different modifications. ..... 22

Figure 2. SEM images of PA (a and b), PA-GO-C (c and d), and PA-GO-Ze-C-PEG (e and f) ..... 23

Figure 3. SEM images of (a) zeolite aggregation, (b) GO + zeolite aggregation, and (c) GO aggregation. ..... 25

Figure 4. Contact angle images of (a) PA, (b) PA-GO-Ze-C, and (c) PA-GO-Ze-C-PEG ..... 27

Figure 5. (a) Water flux and (b) salt rejection of GO embedded membranes.. ..... 29

Figure 6. (a) Water flux and (b) salt rejection of zeolite embedded membranes ..... 31

Figure 7. (a) Water flux and (b) salt rejection of PEG grafted membranes.. ..... 33

Figure 8. Anti-fouling properties of different membranes.. ..... 35

# 1. INTRODUCTION AND BACKGROUND

## 1.1 Research background

It is well-known that Reverse Osmosis (RO) is a popular water treatment during which the dissolved inorganic solids such as various salts can be removed from a solution with a semi-permeable membrane. There are also several other treatments available in the market. When compared with those water treatment methods, RO method is found to be superior due to various reasons. Firstly, in RO process, there is only consumption of electricity. This makes RO more environmentally friendly than other methods like multi-stage flash distillation (MSF), which needs steam and thermal energy.[2] Secondly, the RO process can be utilized in significantly larger water sources where other methods fail and is applicable for sea water reverse osmosis (SWRO), lake water and brackish water reverse osmosis (BWRO) treatment etc. Those advantages make RO one of the most popular water treatment methods.[3]

The most important part in RO technology is the semi-permeable membrane mentioned above. Semi-permeable membrane is a kind of membrane that only allows the transportation of water molecules and rejects ions and solid particles. There are some polymeric membranes, such as polysulfone (PSF) and polyethersulfone (PES) membranes are already commercialized in the market as ultrafiltration membranes. However, these membranes have several problems that limit their further development,

such as low hydrophilicity and short lifetime.[4, 5] For futuristic, a cheap and readily affordable membrane with high reliability water treatment ability is essential.[5] The mechanism and the development of the semi-permeable membrane will be discussed in the following section.

**1.2 Mechanism of reverse osmosis desalination**

There are mainly two ways to separate ions and water molecules by semi-permeable membranes. They are size effect and electricity repulsion effect.

It is easy to understand that the radius difference of water molecules and hydrated ions can be used to separate ions and molecules. Generally, the hydrated ions have the radius of 0.5 nm while the radius of water molecules is about 0.275 nm.[6] However, if we only use the size effect to reject ions, the water flux will not be sufficient for large scale application. Also, the small differences between the radiuses of those ions make it is harder to develop good membranes.

In order to have high water flux and ions rejection at the same time, another phenomenon, Gibbs-Donnan effect is introduced here. This phenomenon is the thermodynamic calculation of the behavior of charged particles near a semi-permeable membrane. In most RO membranes, the selective layer is negatively charged. The negatively-charged ions cannot pass through this negatively-charged membrane.

To understand this phenomenon, we now establish a condition that NaCl and KCl

solutions are on the two sides of the membrane. The concentration of NaCl solution is $c_1$ and that of KCl solution is $c_2$. The membrane itself is negatively charged so $Cl^-$ cannot go through the membrane. After some time, the system will reach equilibrium, the concentration of $Na^+$ decreased $x$ on the side of NaCl solution.

| | | | | | |
|---|---|---|---|---|---|
| *Initial* | $c_1$ | $Na^+$ | | $K^+$ | $c_2$ |
| | $c_1$ | $Cl^-$ | | $Cl^-$ | $c_2$ |
| *Equilibrium* | $c_1 - x$ | $Na^+$ | Membrane | $Na^+$ | $x$ |
| | $x$ | $K^+$ | | $K^+$ | $c_2 - x$ |
| | $c_1$ | $Cl^-$ | | $Cl^-$ | $c_2$ |
| | (1) | | | (2) | |

Then based on the thermodynamic laws, we have following equations.

$$dF = -SdT - PdV + \mu dN + \delta W$$

Equation 1

$$dF = RT\left[\partial n \log\frac{[Na^+]_1}{[Na^+]_2} + \partial n \log\frac{[K^+]_1}{[K^+]_2}\right] = 0$$

Equation 2

After the calculation, we will get the result.

$$\frac{[Na^+]_1}{[K^+]_1} = \frac{[Na^+]_2}{[K^+]_2} = \frac{c_1}{c_2}$$

Equation 3

The result above is also true for a system of salt water and useable water. Equation 3 shows that the salt concentration of two different solutions will hold at equilibrium state. The ions that can travel through the membrane are linearly related to the initial salt concentration. With the Gibbs-Donnan effect, water molecules can be transported from the concentrated side to diluted side while the charged ions are rejected by the semi-permeable membrane. Only applied pressure is needed to overcome the osmotic pressure between the concentrated solution and diluted solution.

Generally, the pressure needed to overcome the osmotic pressure between sea water and usable water is more than 20 bars.[7] This means that we need an additional pressure supply, so a power pump is necessary for the operation of the RO system. This pump will consume most of the energy needed for the RO desalination process. The energy consumption of water is calculated by dividing pump power by water permeability. In order to reach low energy consumption, high water permeability is needed. Another practical problem is the solid particles other than ions. Organic particles can attach to the surface and pores of the membrane because of the hydrophobicity of the membrane and organic foulant.[8] This phenomenon will also decrease the water permeability and increase the energy consumption of the system.

When we put the developed membrane into practice, the anti-fouling property is also important.

### 1.3 Approaches to increase membrane performance

Enormous efforts have been made to increase the water permeability and anti-fouling property of the membrane. Basically, there are two different methods of membrane modification. The first one is the introduction of nanoparticles to the selective layer, mainly by physical attachment. The second one is the surface modification of the selective layer by chemical graft. [9,10,11, 12]

The method that introduces nanoparticles to the selective layer in attempts to enhance the water permeability and anti-fouling property has attracted much attention during the past few years. There are several different introduction methods including functional groups assisted nanoparticles immobilization and interfacial polymerization (IP) assisted nanoparticles immobilization.

The immobilization of nanoparticles (like $TiO_2$) via self-assembly with terminal functional groups on the PA membrane is a method that directly attaches the nanoparticles to the surface of selective membrane. Those immobilized nanoparticles worked as hydrophilic sites and led to good anti-fouling property. Kim et al. decorated the $TiO_2$ nanoparticles on the PA membrane surface by a simple dipping method. They claimed that their fabricated membrane showed a significant higher anti-fouling

property than the pristine membrane.[13] Similar methods and results were reported by other researchers for PES membrane.[14, 15] Other nanoparticles like Ag, sliver nitrate, and copper were also proved to have similar function in enhancing the membrane properties.[16-18]

Another immobilization of nanoparticles is conducted through the IP process. This method is basically embedding the nanoparticles in the selective layer. Mansourpanah et al. proposed a method of embedding GO in the PA layer to increase the water flux and anti-fouling property.[10] Further, Safarpour et al. demonstrated that addition of inorganic particles like $TiO_2$ with reduced GO could improve water flux property.[11] Duan et al. highlighted that the addition of zeolite to the framework of the PA layer could reach a high water flux without decreasing the salt rejection properties.[1] Also, Kim et al. embedded Ag nanoparticles and functionalized multi-walled carbon nanotubes in the membrane. Their membrane showed improved water permeability and anti-fouling property compared with the pristine membrane.[19]

However, problems for nanoparticles immobilization are contradictory. Nanoparticles decorated on the surface are not sufficient for long term operation of the membrane because of the physical bonding while embedded nanoparticles will not be able to enhance the membrane property to the level of surface decoration.

Surface modification of the selective layer is done by attaching macromolecular

chains to the surface of selective membrane by covalent bonds. Popular surface modification methods include UV-graft, Plasma induced grafting, chemical vapor deposition, and direct reaction.

The UV-graft is an approach involves the generation of free radicals from the membrane surface and monomer attachment with the help of UV irradiation. Yamagishi et al, successfully grafted 2-hydroxyethyl methacrylate onto the PES surface. This modified membrane reduced Bovine Serum Albumin (BSA) attachment by 15% compared with the unmodified membrane.[20] Also, Ma et al. claimed a modified membrane by grafting PEG, acrylic acid, and 2-(dimethyl- amino) ethyl methacrylate onto selective layer surface using UV-graft polymerization. Their modified membrane showed higher recovered flux than unmodified membrane.[21] Mansourpanah et al. also used acrylic acid together with UV irradiation to modify PA membrane. A membrane with improved salt rejection and water flux performance was observed.[22] So far, UV-graft has been properly investigated and widely reported.

Plasma induced grafting is similar to UV-graft. Both of them started from the generation of radicals. The advantage of plasma induced grafting is the controlled grafting density and grafted chain length. Yu et al. attached polyvinylpyrrolidone on the polypropylene membrane by using plasma induced grafting. Their result showed that the water flux recovery ratio for the modified membrane was 79% higher than

unmodified membrane.[23] Researches of plasma induced grafting of polyacrylamide onto polyamide membrane were conducted by different groups. All of them observed increase in water flux and anti-fouling property.[24, 25]

The chemical vapor deposition involves the introduction of vapor phase monomer to the surface of the membrane and the direct thin film formation on that membrane. Gleason et al. grafted poly-(sulfobetaine) zwitterionic groups onto commercial membrane by using chemical vapor deposition. Their results showed a 60% increase in water flux as well as good anti-fouling property.[26] Matin et al. also used this method to modify a commercial membrane with 2-hydroxyethyl methacrylate-co-perfluorodecyl acrylate copolymer. When compared with pristine PA membrane, the water flux of the modified membrane is increased by 15%.[27]

However, UV-graft, Plasma induced grafting, and chemical vapor depositions share a same problem. Their high requirement for operational environment and complex fabrication procedure make them hard to be used in large-scale production.

Recently, Choi et al. has developed a layer-by-layer method to coat GO on the surface of the PA membrane by direct reaction between GO and polyamide. Their modified membrane showed great resistance against chlorine.[9] Also, different methods of layer-by-layer assembly were reported, such as the combination of Poly (sodium 4-styrenesulfonate) together with poly (allylamine hydrochloride)[28] and Poly

(styrenesulfonic acid) sodium salt together with poly (diallyldimethylammonium chloride).[29] Both of those modified membranes showed higher water flux and better anti-fouling property than unmodified membranes.

Besides the layer-by-layer assembly, single-layer coating was also reported. Jessica et al. reported the improved anti-fouling property of RO membrane by grafting PEG onto the surface of the PA membrane using potassium persulfate and potassium disulfite as surfactant.[30]

Advantages of this direct reaction coating method are its simple fabrication procedure and low requirement for operational environment. These advantages make the direct reaction coating method a promising alternative method for future research.

**1.4 Motivation and experimental design**

Those two methods mentioned above have different advantages and drawbacks. Researchers mainly concentrated on one of those methods. The reports of multi-modification and simplified fabrication methods are few. It's important to find an advanced method and take the membrane research to a new stage.

In our research, we were trying to solve the anti-fouling and water flux problem by combining the surface modification and nanoparticles introduction together. Inspired by those references mentioned above, we decided to embed nanofillers as water flux channels and decorate surface modification polymers as organic foulant

repelling layer as a beginning. Based on this, we developed a 3-layer structure membrane which includes a PA selective layer filled with nanofillers, an additional GO layer on the top of PA layer, and a PEG anti-fouling layer on the top of GO layer to reach an optimal condition for anti-fouling and water flux property (Scheme 1).

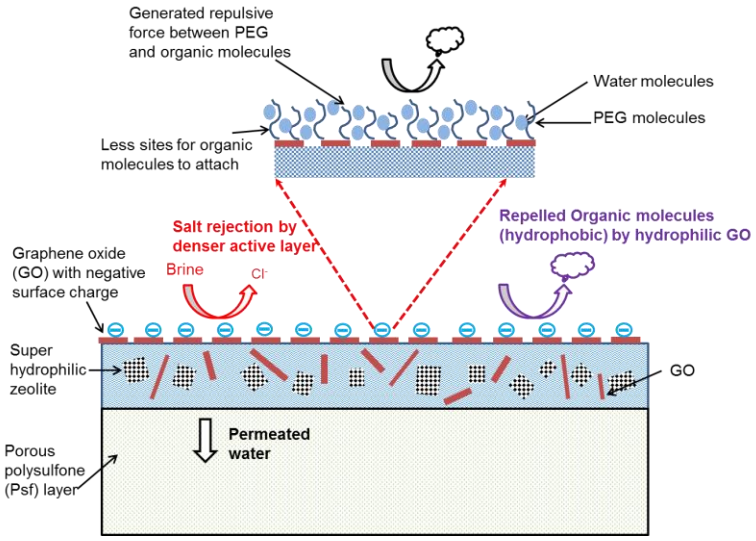


Scheme 1. Schematic illustration of the 3-layer membrane

It was expected that the introduction of nanoparticles into PA layer would increase the water flux. This could be attributed to the super hydrophilic surface of nanoparticles.[31, 32] However, we expected that there would be some compromises between the water flux and some other membrane properties, such as the salt rejection. In addition, some morphology changes caused by the nanoparticles could happen. Firstly, the pores of the selective membrane could be blocked by those additional particles. Those blocked pores could lead to low water permeability property. Secondly, the particles might form clusters and cause the overall salt rejection decrease.[33] Even in

the ideal case, the salt rejection performance would still show slightly decrease due to the molecular-scale voids between the nanoparticles and the polymer. We hypothesized that those two factors would change in an acceptable range and the overall performance would increase.

The role of GO surface coating was expected to be a denser layer which would increase the salt rejection performance and work as the graft position for PEG, but this denser layer would lead to the decrease in water flux because of the longer water transport path created after GO coating. We hoped that the salt rejection would increase and the water flux would not significantly decrease.

The PEG is well known for its extraordinary ability of resisting protein adsorption due to its hydrophilicity, large excluded volume, and unique coordination with surrounding water molecules in an aqueous medium.[34] The schematic illustration is shown in Scheme 2. The PEG molecules are almost neutral and possess no acidic sites except the weak hydrogen-bond acid, hydroxyl groups. The PEG will be heavily hydrated in the water because of the hydrogen binding between hydroxyl groups, ether groups, and water, so the sites for organic molecules to bind are limited. Also, it is reported that when protein approaches towards the PEG, the chains of the PEG will generate a repulsive elastic force because of the compression of PEG chains. Also, the removal of the water molecules from the chains is thermodynamically unfavorable,

which will further repel the organic molecules.[35, 36] The PEG can also further enhance the water flux because the water will be attracted by the PEG. By grafting PEG, we wanted to introduce the great anti-fouling polymer layer onto our membrane and significantly increase the lifetime of the membrane.

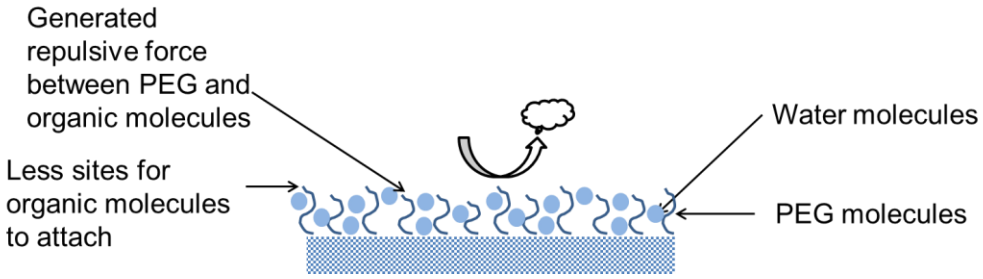


Scheme 2. Schematic illustration of PEG anti-fouling layer

## 2. CHEMICALS AND MATERIALS

The PSF membrane we used here was purchased from Nanostone Water, Inc. Membranes were used as received. The n-hexane, trimesoyl chloride (TMC) and 1, 3-phenylene diamine (MPD) were purchased from Sigma Aldrich and used as received. The Linde type A (LTA) zeolite was purchased from Sigma Aldrich. The certified material reference showed that the median micropore width is 0.59 nm. The LTA zeolite has the Si/Al ratio of 1.0, which leads to negatively-charged surface. The zeolite was milled with 4” extra deep agate mortar (Across International) for further usage. The GO was used as received. The BSA was also purchased from Sigma Aldrich. The BSA was stored under refrigeration before use. The PEG-8000 was purchased from Sigma Aldrich and stored at room temperature.

# 3. EXPERIMENTAL

## 3.1 Zeolite preparation

Zeolite (1mm diameter particles) was milled in the mortar for 1 hour to get small particles. Bath type sonication was used to disperse the fine powder in DI water. After the sonication, the suspension was centrifuged at 8000 RPM for 10 minutes to get the precipitation. The remained top solution was centrifuged for another 10 minutes. Then the remained upper solution was collected and dried overnight at vacuum oven to get dry zeolite powder.

## 3.2 Preparation of PA layer with nanofillers

The schematic illustration of nanofillers decoration is shown in Scheme 3. We were expecting uniformly embedded nanoparticles. It was widely reported that the nanoparticles could be embedded in the polymer layer through the IP process.[1,37]

In this research, the TMC and MPD were used as reagents to activate the IP reaction on a PSF membrane. In detail, the TMC was dissolved in n-hexane with a concentration of 0.15 wt% and the MPD was dissolved in the distilled water with a concentration of 2 wt%. At the same time, the nanofillers GO (0 to 0.5 wt%) and zeolites (0 to 0.08 wt%) were added to the MPD solution with different concentrations to test how those nanofillers would influence the performance of membranes.

The as purchased PSF membrane was immersed in the MPD solution for 1 hour to

fully saturate the pores of the membrane with MPD solution. The treated membrane was taken out and the excess solution on the surface of the membrane was removed. Then the membrane was immersed in TMC solution for two minutes to finish the IP process. This process embedded the nanofillers in the PA selective layer. After the IP process, the membrane was rinsed with DI water. Prepared membranes were stored in DI water before further treatment.

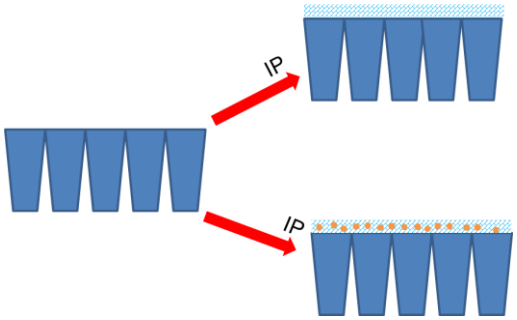


Scheme 3. Schematic illustration of nanoparticles decoration

**3.3 Surface modification of PA layer with GO layer**

The GO could be coated on the surface of the polyamide selective layer by the reaction between the functional groups on GO and PA. The mechanism schematic is shown in Scheme 4. The two monomer chemicals shown in (a) and (b) are TMC and MPD. After the IP process, the remained –COCl groups on the surface of GO would react with the –OH through equation 4. This chemical bonding would generate a uniform layer of GO on the surface of PA selective layer.

$$OH + -COCl \rightarrow -COO + HCl \qquad \text{(Equation 4)}$$

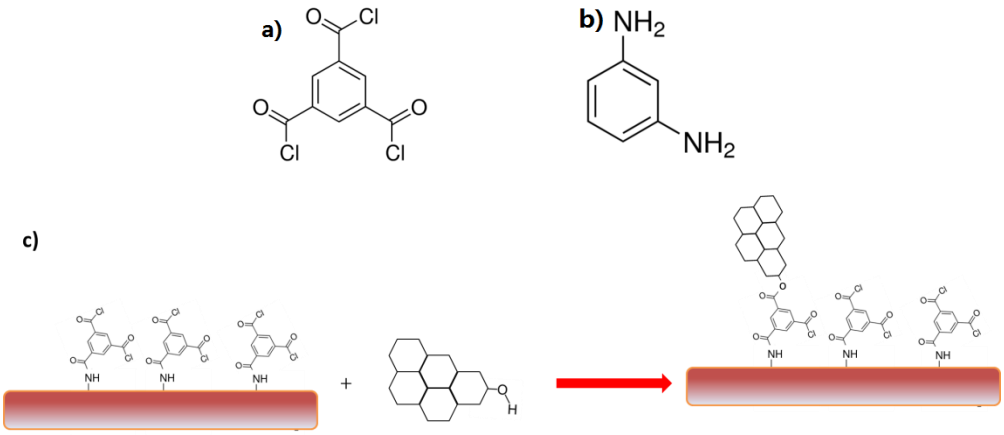


Scheme 4. (a) TMC, (b) MPD, and (c) schematic illustration of the GO coating mechanism[8]

In this research, we achieved the reaction by immersing the membrane into the GO solution (0.05 wt%) for 1 hour to finish the reaction between functional groups of PA and GO. After that, the membrane was rinsed with DI water to remove the excess solution.

### 3.4 Surface modification of GO layer with PEG layer

The PEG layer was grafted on the surface of GO by the reaction between –OH groups of PEG and –COOH groups of GO. The chemical structure of the reaction product is shown in Scheme 5.

The PEG aqueous solution was prepared with the concentration of 50 wt%. The dried GO coated membrane was soaked in the PEG solution for 24 hours. After the reaction, the membrane was rinsed with DI water and stored in DI water for further

test.

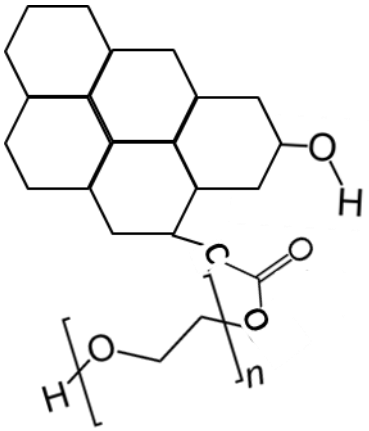


Scheme 5. Chemical structure of PEG modified GO

After the preparation of the membranes, we got 7 different types of membranes. They were named in Table 1

Table 1. List of samples

| Name | Nanofillers | Coat | Graft |
|---|---|---|---|
| PA | | | |
| PA-Ze | Zeolite (0 to 0.08 wt%) | | |
| PA-GO | GO (0 to 0.5 wt%) | | |
| PA-Ze-C | Zeolite (0 to 0.08 wt%) | GO | |
| PA-GO-C | GO (0 to 0.5 wt%) | GO | |
| PA-GO-Ze-C | GO (0 to 0.5 wt %), Zeolite (0.04 wt %) | GO | |
| PA-GO-Ze-C-PEG | GO (0 to 0.5 wt %), Zeolite (0.04 wt %) | GO | PEG |

### 3.5 Characterization methods of nanofillers and membranes

FTIR characterization results were collected using fourier transform infrared (ATR-FTIR) spectrometer (Shimadzu IR Prestige). Film samples were prepared before the FTIR characterization.

The zeta potential was tested to confirm the zeta potential change of the graphene oxide before and after the PEG modification. The reaction between the functional groups on GO and PEG would consume the -COOH of the GO. The consumption of those functional groups would lead to the reduction of zeta potential. This might

potentially decrease the salt rejection rate of the membrane.

The zeta potential results were collected with DelsaNano C DLS. The GO+PEG suspension was prepared before testing. Firstly, we dissolved 45 mg GO and 10g PEG in 20 mL DI water. Then the result suspension was sonicated for 24 hours to finish the reaction. After reaction, the solution was centrifuged under 8000 RPM for 30 minutes. The precipitation was collected and washed with DI water. Then the precipitation was dissolved again and went through this process for 3 times to fully remove the excess PEG in the solution. Then the GO+PEG was dissolved in DI water. The GO solution was prepared by dispersing GO into DI water. The pH values of these solutions were adjusted to 7 before zeta potential tests.

In order to investigate the structures of the membrane and confirm the attachment of GO and PEG, SEM images was collected with JEOL JSM-7500F. The samples were coated with platinum before taking SEM images to avoid the surface charge of the insulating polymer surface. Besides this, the aggregation of nanoparticles was also characterized by drying zeolite solution, GO solution, and GO + Zeolite solution on a copper foil. Images of the dried particles were taken using SEM to observe the aggregation tendency.

The contact angle results were characterized by using high pixels camera. The images were enlarged and contact angles were measured based on that.

### 3.6 Performance and fouling characterization methods

The membrane was assembled into a homemade cross-flow equipment to test the water flux. The salt solution was NaCl solution (0.35 wt%) and the applied pressure was 250 Psi.

After collecting the permeated water from the setup, the conductivity of the permeated water was tested by a conductivity meter (Iso Pod, Australia). The salt rejection rate was calculated by using the conductivity & concentration chart.

The anti-fouling property was tested with the same equipment. The test solution was BSA aqueous solution with a concentration of 0.01 wt%. Water flux was tested at the beginning, 2 hours, 4 hours and 6 hours of the experiment. After 6 hours, the membrane was taken out and cleaned with DI water for 5 minutes. The membrane was tested again to get the recovery rate (water flux after cleaning / initial water flux).

# 4. RESULTS AND DISCUSSION

## 4.1 Characterization results of membranes

The FTIR results are shown in Figure 1. Two new peaks were observed at 1541 $cm^{-1}$ and 1667 $cm^{-1}$ after IP process. These two peaks were attributed to the PA skin layer on the PSF support.[38] The peak at 1541 $cm^{-1}$ was due to the N-H in-plane bending and N-C stretching vibration of a -CO-NH- group. The peak at 1667 $cm^{-1}$ was assigned to the C=O stretching vibration in a secondary amide group.[38] These peaks confirmed the successful IP process.

For the GO layer modification and PEG layer modification, it was hard to directly get information from the peak location results. However, information could still be found from the relative peak intensity information. As can be seen, the peak intensity at 1090 $cm^{-1}$ and 1150 $cm^{-1}$ (Figure 1) varied a lot during the GO and PEG modification process. The peaks at 1090 $cm^{-1}$ and 1150 $cm^{-1}$ could be the -C-O stretching vibrations near the aromatic C=C bonds and -C-O near -C-C bonds, which corresponded to GO and PEG.[39] The increased ratio of Peak 1 and Peak 2 could be explained by the introduction of aromatic C=C bonds together with GO. In that case, the overall -C-O near the aromatic C=C groups increased while the -C-O near -C-C bonds remained constant. After grafting PEG, the ratio became low again due to the large amount of -C-C- bonds on PEG molecules. The graft of PEG increased the amount of -C-O near

-C-C bonds on the surface of membrane and led to the observed peak change. This result supported the proposed reaction between PA, GO and PEG in each different membrane layer. FTIR results showed the evidence of successful surface modification. The SEM images also confirmed the success of GO and PEG modification on the surface of the membrane, which are shown below.

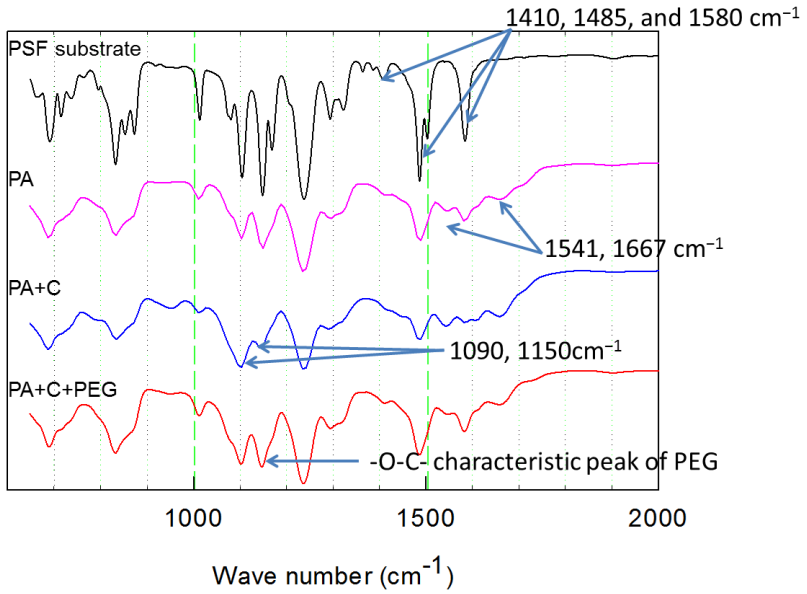


Figure 1. FTIR results of membranes with different modifications

SEM images of different samples are shown in Figure 2. As we can see from the results, there were clear GO coating and PEG grafting on the surface of the membrane. The GO layer and PEG layer also led to change of the surface morphology between pristine PA membranes, GO coated membrane, and PEG grafted membrane.

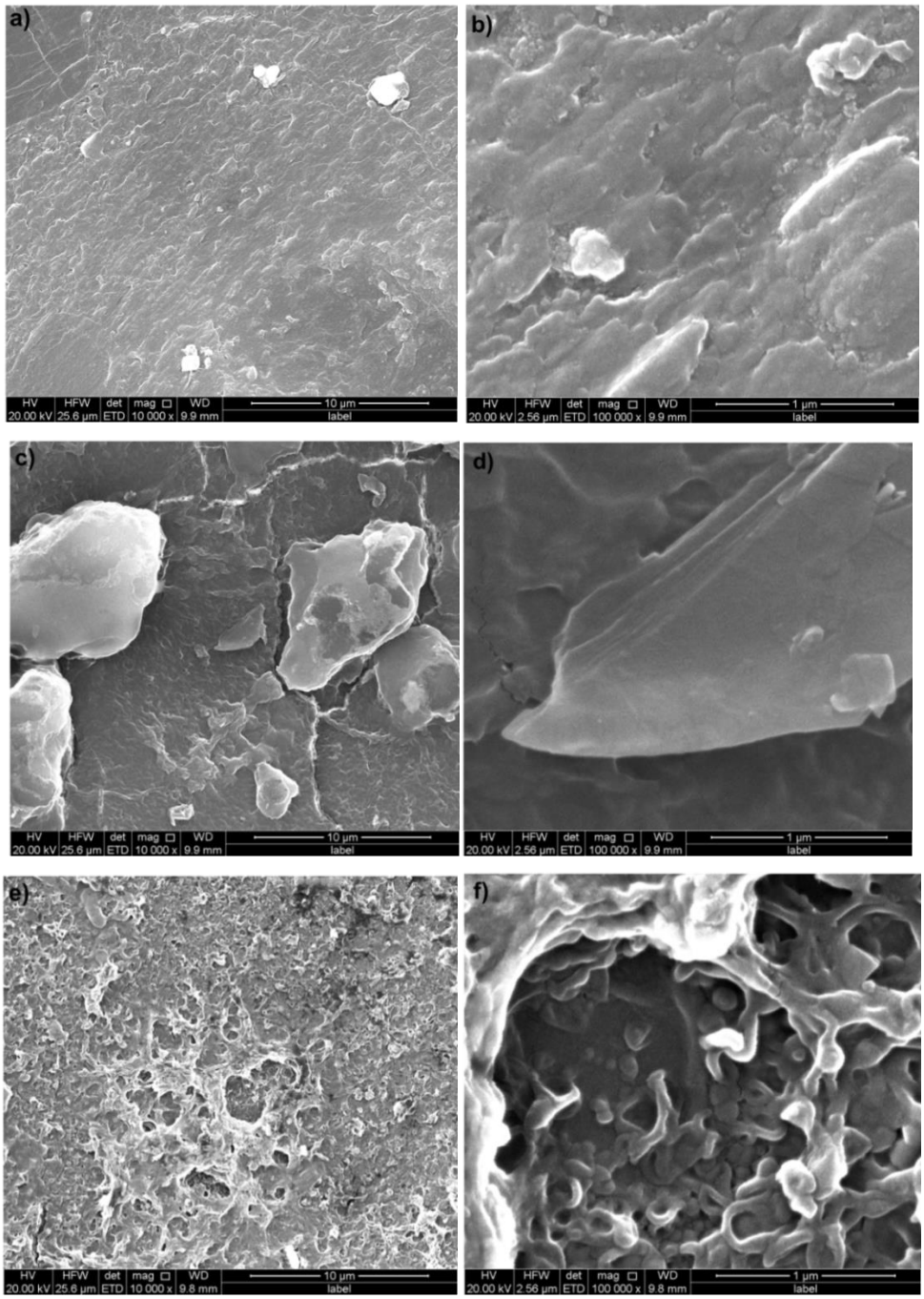


Figure 2. SEM images of PA (a and b), PA-GO-C (c and d), and PA-GO-Ze-C-PEG (e and f)

Also, images of nanoparticles aggregation are shown in Figure 3. The

concentration of GO and zeolite used here was the same with the GO and zeolite concentration in MPD solution. We calculated the pixels of the zeolite particles we could find on the image. (Figure 3 a, b red square) The number of pixels of zeolite image was 38966 while that was 41382 for zeolite + GO image. This showed that the particles densities were the same in two samples. At the same time, the particle number was 32 for zeolite sample and 49 for zeolite + GO sample. This result showed that the aggregation was reduced when adding GO and zeolite together into the solution. The reason could be the surface charge of GO and zeolite. The same surface charge made them repelling each other. This aggregation result showed the tendency of aggregation behaviors of nanoparticles in the selective membrane layer. This decreased aggregation could lead to a membrane with few defects and high salt rejection.

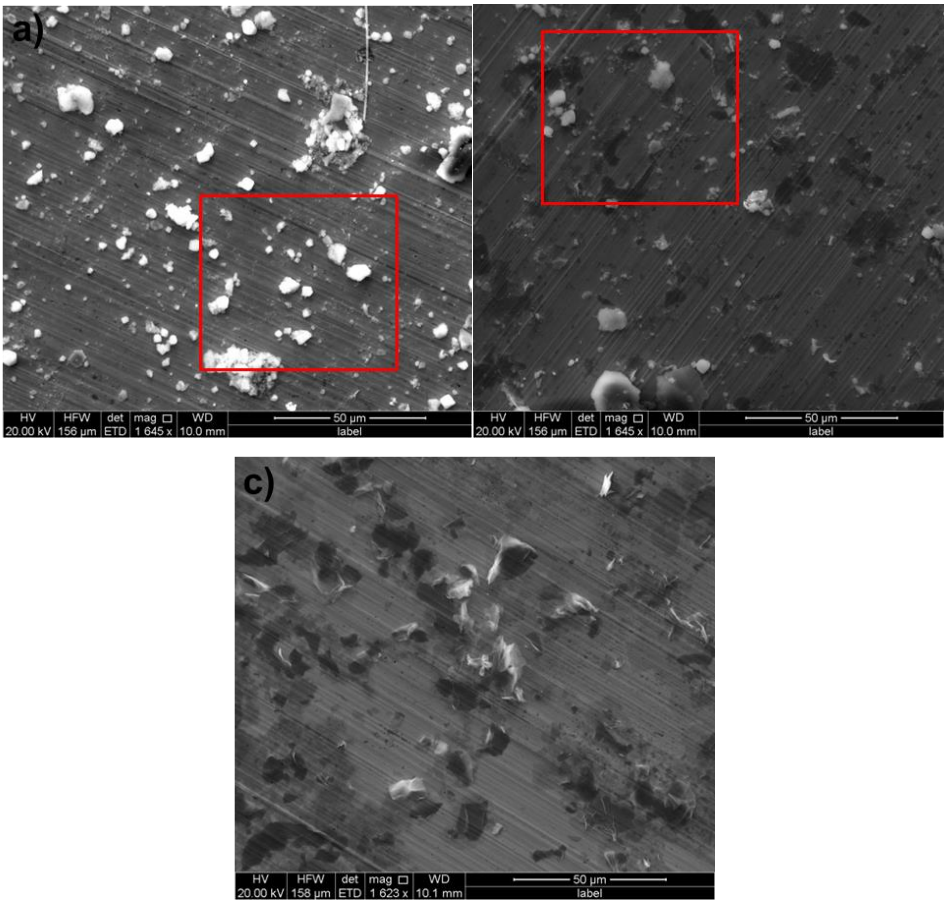


Figure 3. SEM images of (a) zeolite aggregation, (b) GO + zeolite aggregation, and (c) GO aggregation

The contact angle images of pristine membrane, GO coated membrane, and PEG grafted membrane are shown in Figure 4. The measured contact angles of different examples are shown in Table 2.

Table 2. Contact angles of different samples

| Name | Contact angle ($^{o}$) |
|---|---|
| PA | 62.3 ($\pm$1.767) |
| PA-GO(0.3%)- Ze(0.04%)-C | 55.5 ($\pm$1.875) |
| PA-GO(0.3%)-Ze(0.04%)-C-PEG | 44.4 ($\pm 2$) |

The contact angle decreased from 62.3 $^{o}$ to 55.5 $^{o}$ after the GO modification. This result is similar to the finding of Liu et al.[40] In their researches, they tested GO embedded PA membrane with 0.6 wt% concentration, which reduced the contact angle from 63.74 $^{o}$ to 55.04 $^{o}$. In another research, PA membrane with GO loading from 0.25 wt% to 15 wt% was tested by He et al. With the increased GO loading, the contact angle decreased from 68 $^{o}$ to 57 $^{o}$.[41] As mentioned before, this contact angle change was attributed to the hydrophilicity of nanoparticles. After grafting PEG onto the surface of GO, we observed the decrease of contact angle which was from 55.5 $^{o}$ to 44.4 $^{o}$. This was also because of the hydrophilic property of grafted PEG.

The reduction of the contact angle showed a successful surface modification. This result also partly explained increase of the water flux and anti-fouling performance in

those modified samples.

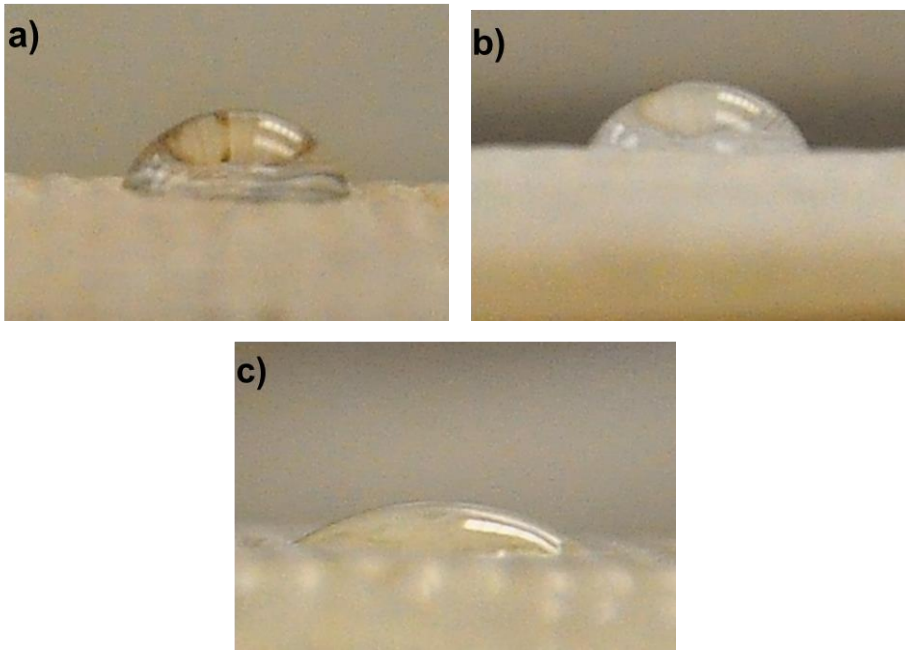


Figure 4. Contact angle images of (a) PA, (b) PA-GO-Ze-C, and (c) PA-GO-Ze-C-PEG

**4.2 Membrane performance and antifouling properties**

The water flux and salt rejection of different samples are shown below. The results of PA-GO series samples are shown in Figure 5. According to the result, PA-GO membrane showed an increased water flux and decreased salt rejection when compared with pristine membrane. The water flux increased from 4.6 $L/m^2/h/bar$ to 10.6 $L/m^2/h/bar$. At the same time, the salt rejection rate decreased from 98.5% to 94%. This increase in the water flux could be explained by the defects created on the PA layer due to GO introduction. Those defects worked as new water flux channels and increased both water and salt permeability. When the GO concentration was further increased,

the salt rejection rate decreased more. The first possible reason could be the increasing defects concentration that made more channels for salt to permeate. Another possible explanation could be that higher GO concentration led to a higher possibility of GO aggregation. The GO aggregation may lead to larger defects and voids for water molecules and salt ions to pass.

When the GO layer was added to the membrane, the salt rejection increased and water flux decreased. When the GO concentration was 0.1%, the salt rejection increased from 95.5% to 96.3% and the water flux decreased from 7.8 $L/m^2/h/bar$ to 6.0 $L/m^2/h/bar$. The decreased water flux was caused by the thicker selective layer. The salt rejection change could also be attributed to the GO layer. Different from the embedded GO, the GO layer had a negatively-charged surface without many defects for salt to permeate. In this case, PA-GO-C showed a good salt rejection rate and reasonable water flux.

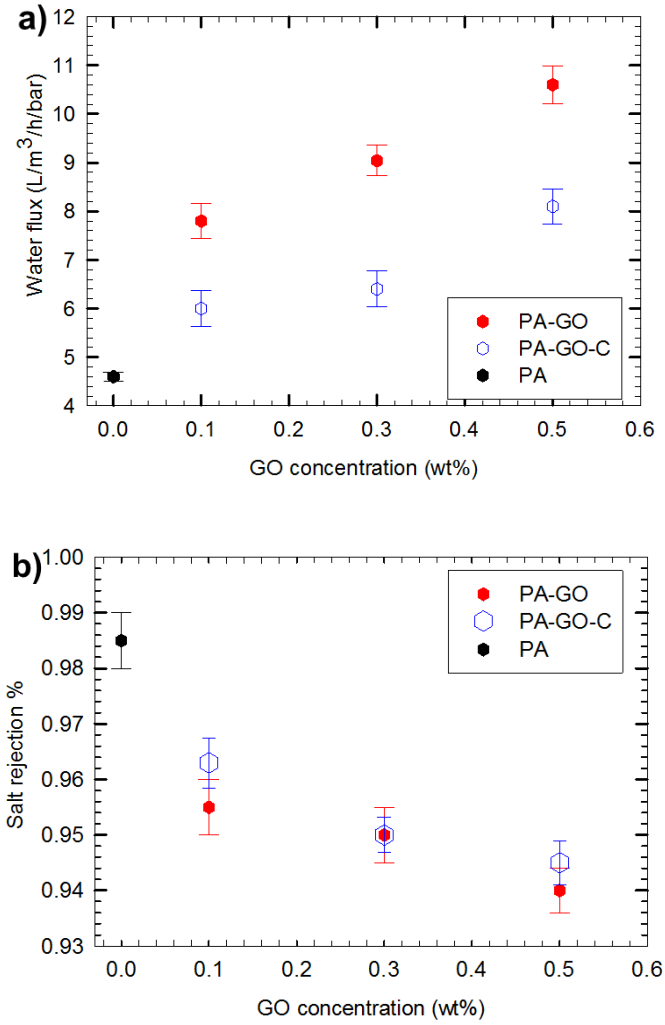


Figure 5. (a) Water flux and (b) salt rejection of GO embedded membranes

When zeolite was added to the membrane (Figure 6 a, b), the water flux increased from 4.6 L/m$^2$/h/bar to 7.3 L/m$^2$/h/bar at zeolite concentration of 0.04% and to 14.02/m$^2$/h/bar at zeolite concentration of 0.08%. At the same time, the salt rejection decreased from 98.5% to 98.1% at the concentration of 0.04%. When the zeolite concentration was 0.08%, the salt rejection decreased to 95.1% (Figure 6). The overall

high performance at zeolite concentration of 0.04% was mainly because of high zeta potential and water flux channel property of zeolite. However, when the concentration was increased, the more voids between zeolite and PA layer and possible zeolite aggregation led to higher salt permeability, which was similar to the situation of GO modification.

For the zeolite embedded membrane with GO layer, similar to the situation of GO modification, small increase in salt rejection and decrease in water flux were observed. At the zeolite concentration of 0.04 wt%, the water flux was 6.72 $L/m^2/h/bar$ and the salt rejection was 98.5%.

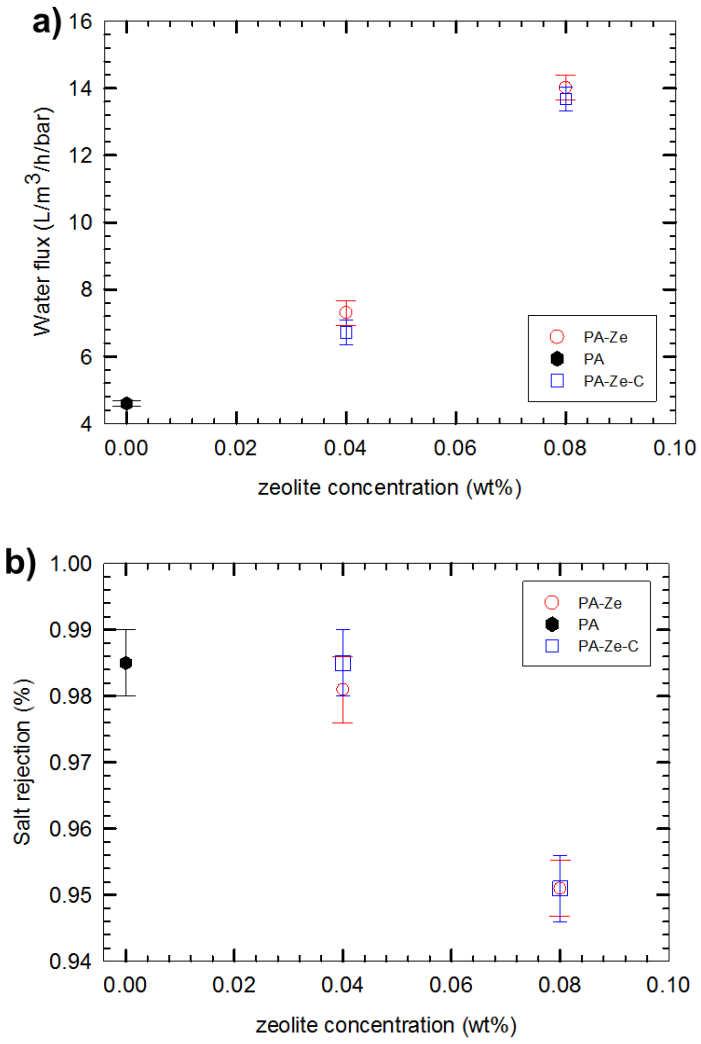


Figure 6. (a) Water flux and (b) salt rejection of zeolite embedded membranes

When we added zeolite and GO together to the membrane, as shown in Figure 7, interestingly, the water flux showed a higher value than that of PA-Ze and PA-GO. After adding the 0.04% zeolite, at the GO concentration of 0.1%, the water flux increased to 11 L/m$^2$/h/bar and the salt rejection maintained the value of 98.3%.

The overall high performance of PA-GO-Ze-C membrane could be attributed to

the individual zeolite and GO decoration as well as the interaction between zeolite and GO. As mentioned before, the zeolite had a higher surface charge than GO, which help rejecting the salt ions. Also, the super hydrophilic zeolite worked as flux channel that increased the water flux together with GO. What's more, both zeolite and GO showed a negatively-charged surface, which gave rise to their tendency of repelling each other. Because of this, the aggregation and defects were reduced. When GO concentration was increased, the decreased zeolite/GO ratio could not hinder the aggregation of GO. This led to the decrease of salt rejection like the PA-GO series membrane.

By grafting PEG (PA-GO-Ze-C-PEG) on the surface of the membrane, we observed that the salt rejection of PA-GO-Ze-C-PEG was lower than that of PA-GO-Ze-C. At GO concentration of 0.3%, the salt rejection of the PA-GO-Ze-C-PEG decreased to 95.8%. The decreased salt rejection was probably caused by the reaction between GO and PEG. This reaction consumed -COOH groups on GO, which led to the reduction of the surface charge. This surface charge reduction was already shown during the zeta potential discussion. Besides decrease of the salt rejection, the water flux showed increase when PEG was coated, the water flux increased from 11.9 $L/m^2/h/bar$ to 13.2 $L/m^2/h/bar$ This result consisted with the claim of Zhao et al.[42] However, the reason of this water flux increase was not discussed in those literatures. The possible reason could be the super hydrophilic property of PEG.

PEG contains ether functional group in every repeat unit, which makes it easy to form hydrogen bond between ether and water molecules. In our research, water molecules were attracted to the surface by PEG modification and water flux was increased.

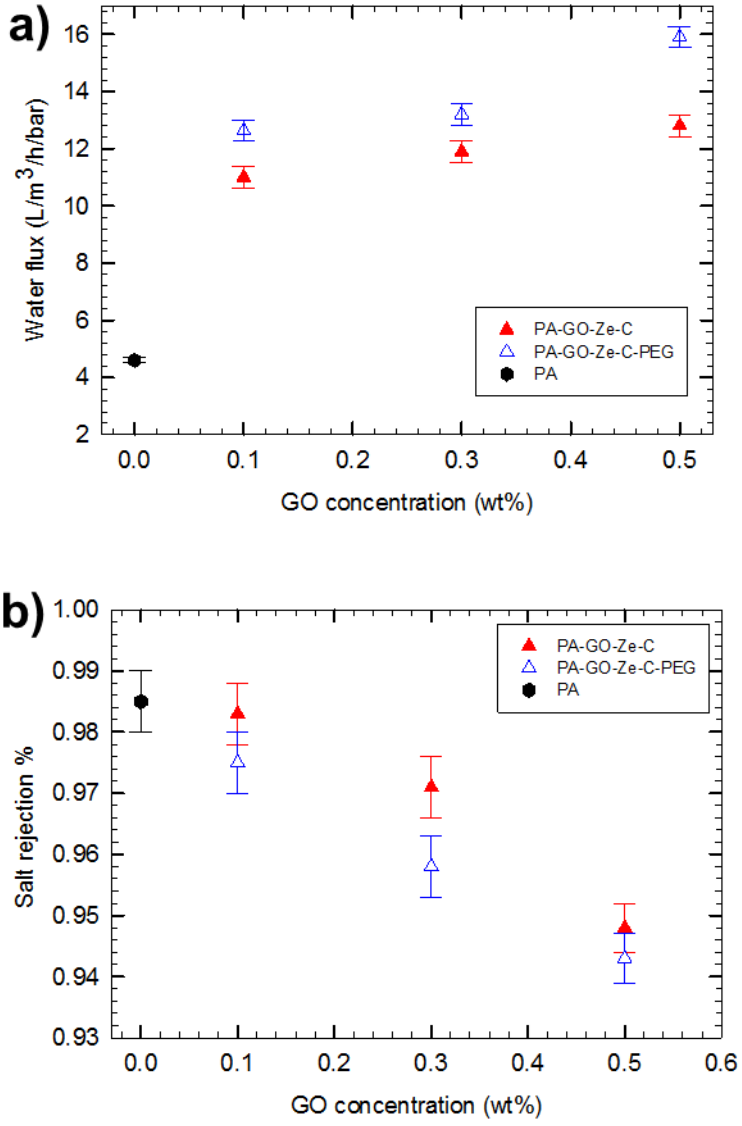


Figure 7. (a) Water flux and (b) salt rejection of PEG grafted membranes

Figure 8 shows the anti-fouling characterization with the normalized water flux

(real flux/initial flux) of membranes after operation time of 2, 4, 6 hours. After 6 hours, the membrane was washed with DI water to remove the organic foulant. The water flux of the cleaned membrane was tested again. As can be clearly seen from the result, the membranes with PEG modification showed a better anti-fouling performance against BSA and a better water flux recovery rate than pristine membranes. The normalized water flux of pristine PA membrane decreased to 70% after 6 hours and recovered to 80% after cleaning. The GO coated membrane showed slightly increased anti-fouling performance after 2 hours. The normalized water flux increased about 5% than the pristine membrane. It's also interesting that the coated membrane showed a high recovery rate after washing. This could be attributed to the flat and hydrophilic surface of GO layer, which led to the easy detachment of organic foulant when washed with DI water.

At the same time, PEG grafted membrane maintained more than 80% normalized water flux after 6 hours operation. After the cleaning, the PEG grafted membrane reached a normalized water flux of more than 87%.

Despite the lower salt rejection, fouling test results showed that the PEG graft could largely improve the anti-fouling property (Figure 8). The largely-improved anti-fouling property made the little decrease in salt rejection a reasonable trade-off. When compared with other literature results, our membrane showed higher potential in

both water flux and anti-fouling properties.

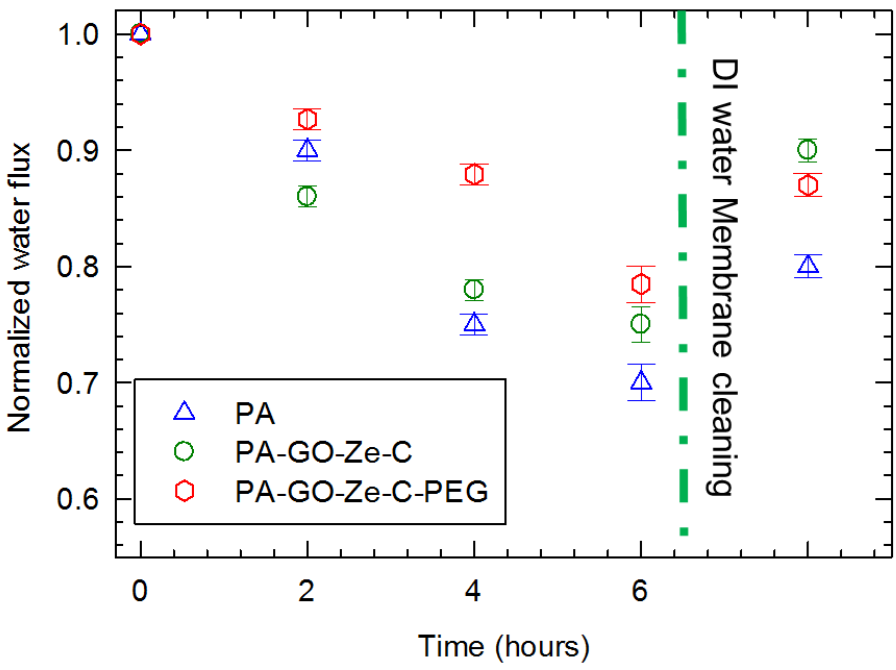


Figure 8. Anti-fouling properties of different membranes

## 5. CONCLUSION AND FUTURE WORK

The impacts of nanofillers and surface modification have been investigated in this research. Results showed that the fabricated 3-layers structure modification could decrease the contact angle from 62.3$^{o}$ to 44.4$^{o}$. We also observed an impressive improvement in water flux from 4.6 L/m$^2$/h/bar to 13.2 L/m$^2$/h/bar. At the same time, the salt rejection was still maintained within an acceptable range. Results also revealed that the anti-fouling performance was largely improved by surface modification. The GO layer used in this membrane helped the introduction of PEG. At the same time, the GO layer itself could improve the membrane performance. This was not reported in other literatures using surfactant. What's more, the fabrication process was easy and no special chemicals were needed for this low-cost technique. This added a huge advantage to the 3-layer membrane with regard to mass production.

When compared with other recent research results, our 3-layer membrane shows a better performance in terms of water flux and salt rejection. The comparison is shown in Table 3.

In the future, further material characteristic jobs and membrane development should be done:

• Nanoparticles aggregation analysis

The BET analysis can determine the specific surface area of aggregated

nanoparticles. This test result will further support our hypothesis of particles aggregation. The evidence we used in this paper is not really sufficient enough to support our aggregation hypothesis.

• Membrane performance characterization

The fabricated membranes will be sent to labs of cooperator in Qatar to further confirm the results we got in our lab.

In order to further describe the advantages of the new fabricated membrane, the traditional PEG grafted membrane using UV-graft or plasma induced grafting will be tested. The purpose of doing this experiment is to confirm that our “surfactant” GO also contributes to the membrane performance.

• Composite optimization

We will change the composition of nanoparticles to find more possible optimal conditions.

• Future research

In this research, we fabricated an advanced membrane with improved water flux and anti-fouling property. In the future, it’s also important to investigate and enhance the anti-bacteria performance of the membrane because bacteria were not included in this research. Also, the membrane fabrication method used in this research can be used to develop other membranes for pressure retarded osmosis and forward osmosis. We

hope that this kind of multi-layer structure fabrication can lead to membrane development to a new stage.

Table 3. Comparison of RO membranes from literature

| Name | Water flux | Salt rejection | reference |
|---|---|---|---|
| 3-layer modified membrane | 13.2 L/$m^2$/h/bar | 95.8% | This research |
| AgNPs embedded membrane | 3.4 L/$m^2$/hr/bar | 93.4% | Yin, Jun, et al.[43] |
| GO sublayer adjusted membrane | 4-8L/$m^2$/hr/bar | 99.3% | Liu, Qian, et al.[40] |
| Hyperbranched polyester enhanced membrane | 11 L/$m^2$/hr/bar | 98% | Kong, Xin, et al.[44] |
| Sulfonated Polyamide Thin-Film | 12.1L/$m^2$/h/bar | 92.5% | Lv, Zhiwei, et al.[45] |
| surface modification via covalent attachment of polyvinyl alcohol (PVA) | 6.16L/$m^2$/h/bar | 98.45% | Hu, Yutao, et al.[46] |

## REFERENCES


1. J. Duan, Y. Pan, F. Pacheco, E. Litwiller, Z. Lai and I. Pinnau, *Journal of Membrane Science*, 2015, **476**, 303-310.
2. N. Ghaffour, S. Lattemann, T. Missimer, K. C. Ng, S. Sinha and G. Amy, *Applied Energy*, 2014, **136**, 1155-1165.
3. C. Zhao, X. Xu, J. Chen and F. Yang, *Journal of Environmental Chemical Engineering*, 2013, **1**, 349-354.
4. A. V. Penkova, M. E. Dmitrenko, M. P. Sokolova, B. Chen, T. V. Plisko, D. A. Markelov and S. S. Ermakov, *Journal of Materials Science*, 2016, **51**, 7652-7659.
5. T. Hwang, J.-S. Oh, W. Yim, J.-D. Nam, C. Bae, H.-i. Kim and K. J. Kim, *Separation and Purification Technology*, 2016, **166**, 41-47.
6. A. Picard, R. Davis, M. Gläser and K. Fujii, *Metrologia*, 2008, **45**, 149.
7. W. Luo, F. I. Hai, W. E. Price, M. Elimelech and L. D. Nghiem, *Journal of Membrane Science*, 2016, **514**, 636-645.
8. E. Igbinigun, Y. Fennell, R. Malaisamy, K. L. Jones and V. Morris, *Journal of Membrane Science*, 2016, **514**, 518-526.
9. W. Choi, J. Choi, J. Bang and J.-H. Lee, *ACS Applied Materials & Interfaces*, 2013, **5**, 12510-12519.

10. Y. Mansourpanah, H. Shahebrahimi and E. Kolvari, *Chemical Engineering Research and Design*, 2015, **104**, 530-540.

11. M. Safarpour, A. Khataee and V. Vatanpour, *Journal of Membrane Science*, 2015, **489**, 43-54.

12. S. K. Lim, L. Setiawan, T.-H. Bae and R. Wang, *Journal of Membrane Science*, 2016, **501**, 152-160.

13. S. H. Kim, S.-Y. Kwak, B.-H. Sohn and T. H. Park, *Journal of Membrane Science*, 2003, **211**, 157-165.

14. M.-L. Luo, J.-Q. Zhao, W. Tang and C.-S. Pu, *Applied Surface Science*, 2005, **249**, 76-84.

15. T.-H. Bae, I.-C. Kim and T.-M. Tak, *Journal of Membrane Science*, 2006, **275**, 1-5.

16. W. L. Chou, D. G. Yu and M. C. Yang, *Polymers for Advanced Technologies*, 2005, **16**, 600-607.

17. F. Rispoli, A. Angelov, D. Badia, A. Kumar, S. Seal and V. Shah, *Journal of Hazardous Materials*, 2010, **180**, 212-216.

18. D.-G. Yu, M.-Y. Teng, W.-L. Chou and M.-C. Yang, *Journal of Membrane Science*, 2003, **225**, 115-123.

19. E.-S. Kim, G. Hwang, M. G. El-Din and Y. Liu, *Journal of Membrane Science*,

2012, **394**, 37-48.

20. H. Yamagishi, J. V. Crivello and G. Belfort, *Journal of Membrane Science*, 1995, **105**, 237-247.

21. H. Ma, R. H. Davis and C. N. Bowman, *Macromolecules*, 2000, **33**, 331-335.

22. Y. Mansourpanah and E. Momeni Habili, *Journal of Membrane Science*, 2013, **430**, 158-166.

23. H.-Y. Yu, Z.-K. Xu, Y.-J. Xie, Z.-M. Liu and S.-Y. Wang, *Journal of Membrane Science*, 2006, **279**, 148-155.

24. K. J. Varin, N. H. Lin and Y. Cohen, *Journal of Membrane Science*, 2013, **446**, 472-481.

25. K. J. Moses and Y. Cohen, *Journal of Colloid and Interface Science*, 2014, **436**, 286-295.

26. R. Yang, J. Xu, G. Ozaydin-Ince, S. Y. Wong and K. K. Gleason, *Chemistry of Materials*, 2011, **23**, 1263-1272.

27. A. Matin, H. Shafi, M. Wang, Z. Khan, K. Gleason and F. Rahman, *Desalination*, 2016, **379**, 108-117.

28. T. Ishigami, K. Amano, A. Fujii, Y. Ohmukai, E. Kamio, T. Maruyama and H. Matsuyama, *Separation and Purification Technology*, 2012, **99**, 1-7.

29. R. Malaisamy, A. Talla-Nwafo and K. L. Jones, *Separation and purification*

*technology*, 2011, **77**, 367-374.

30. J. R. Ray, S. Tadepalli, S. Z. Nergiz, K.-K. Liu, L. You, Y. Tang, S. Singamaneni and Y.-S. Jun, *ACS applied Materials & Interfaces*, 2015, **7**, 11117-11126.

31. S. Bano, A. Mahmood, S.-J. Kim and K.-H. Lee, *Journal of Materials Chemistry A*, 2015, **3**, 2065-2071.

32. H. M. Hegab and L. Zou, *Journal of Membrane Science*, 2015, **484**, 95-106.

33. L.-x. Dong, X.-c. Huang, Z. Wang, Z. Yang, X.-m. Wang and C. Y. Tang, *Separation and Purification Technology*, 2016, **166**, 230-239.

34. X. Ma, Y. Su, Q. Sun, Y. Wang and Z. Jiang, *Journal of Membrane Science*, 2007, **292**, 116-124.

35. J. M. Harris, in *Poly (ethylene glycol) Chemistry*, Springer, 1992, pp. 1-14.

36. I. Banerjee, R. C. Pangule and R. S. Kane, *Advanced Materials*, 2011, **23**, 690-718.

37. H. Huang, X. Qu, H. Dong, L. Zhang and H. Chen, *RSC Advances*, 2013, **3**, 8203-8207.

38. Y. Wang, X. Li, C. Cheng, Y. He, J. Pan and T. Xu, *Journal of Membrane Science*, 2016, **498**, 30-38.

39. S. Yu, J. Liu, W. Zhu, Z.-T. Hu, T.-T. Lim and X. Yan, *Scientific Reports*, 2015,

**5**.

40. Q. Liu and G.-R. Xu, *Desalination*, 2016, **394**, 162-175.

41. L. He, L. F. Dumée, C. Feng, L. Velleman, R. Reis, F. She, W. Gao and L. Kong, *Desalination*, 2015, **365**, 126-135.

42. L. Zhao, P. C.-Y. Chang, C. Yen and W. W. Ho, *Journal of Membrane Science*, 2013, **425**, 1-10.

43. J. Yin, Y. Yang, Z. Hu and B. Deng, *Journal of Membrane Science*, 2013, **441**, 73-82.

44. X. Kong, Y. Zhang, S.-Y. Zeng, B.-K. Zhu, L.-P. Zhu, L.-F. Fang and H. Matsuyama, *Journal of Membrane Science*, 2016, **518**, 141-149.

45. Z. Lv, J. Hu, J. Zheng, X. Zhang and L. Wang, *Industrial & Engineering Chemistry Research*, 2016, **55**, 4726-4733.

46. Y. Hu, K. Lu, F. Yan, Y. Shi, P. Yu, S. Yu, S. Li and C. Gao, *Journal of Membrane Science*, 2016, **501**, 209-219.